

Effect of Sodium Based Transparent Binders on the Optical Properties of GaSe Thin Films

Ahmad Omar

Department of Physics, Arab-American University- Palestine

ahmad.omar@aauj.edu

Abstract

The effect of sodium based transparent binders on the optical properties of vacuum evaporated GaSe thin films are explored by means of optical reflectivity and transmittance of the binder, GaSe and GaSe/binder interfaces in the incident light wavelength range of 300-1100 nm. The analysis of the absorption coefficient spectra for the three samples revealed a pronounced red shift in the direct allowed electron transition's energy band gap of the GaSe. In addition, the band tail states of GaSe, which was observed at ~ 0.25 eV, disappeared upon binder coating. The binder coated GaSe films screen the energy band gap of the GaSe as band tail state in its energy band gap. On the other hand, the analysis of the dielectric spectra of the binder coated GaSe thin films displayed an abnormal enhancement in the optical conductivity of the double layer. The optical conductivity, which was modeled in accordance to Lorentz theory, displayed significant change in the free carrier density, the drift mobility, the electron collision time and the effective mass of GaSe upon binder coating. The study ends with the result that the sodium-based binder behaves as a fully transparent optical window to the optoelectronically sensitive GaSe thin films.

Keywords: *Optical Conductivity, Binder, Coating, GaSe*

Introduction

The importance of GaSe in scientific research and applied sciences is due mainly to its distinguished electronic, structural and optical characteristics. Applications of GaSe in the visible range of the electromagnetic spectrum is promising (Qasrawi, 2005).

Measurements of the absorption coefficient and refractive index for samples of GaSe prepared at low temperature near the band edge have been reported (Toullec et al., 1980). The position and intensity of the exciton's levels using Elliott's model in performing the necessary fit make it possible to estimate the values of the band gap, excitons binding energy, the excited levels damping, the strength of the oscillator transition, in addition to the reduced masses of the exciton. S. Shigetomi and T. Ilkari concluded that the excess Ga and Se atoms in GaSe samples cause the indirect band transition (Shigetomi, and Ikari, 2003). The optical properties and applications of effective nonlinear GaSe crystal is reviewed, discussed and studied thoroughly by using confocal Raman spectroscopy experiments. The prominent views for future research on GaSe are considered (Allakhverdiev et al., 2009).

In this article, we analyzed the transmission and reflection spectra, which is helpful in investigating the variation of the real and imaginary parts of the dielectric constant and the absorption coefficient as functions of frequency for GaSe/Binder thin film. These analyses are necessary in investigating and evaluating the rule of optical conductivity for GaSe/Binder double layer thin film. Optical conductivity relates the current density, in the illuminated material and the incident photon electric field. Since optical conductivity represents the response of thin films to electromagnetic spectrum, it proves to be a powerful method for measuring the electronic states of materials (Schrieffer, 2007). The real part of the optical conductivity represents the damping of the electromagnetic energy in the material, while the imaginary part represents the screening of the applied field (Schrieffer, 2007). Optical conduction in amorphous GaSe thin films is explored and reported. Amorphous GaSe thin films are observed to follow the Lorentz model for optical conduction (Qasrawi et al., 2016).

As the GaSe is a photovoltaic semiconductor and used for solar energy harvesting it should be protected from natural atmospheric conditions like humidity, which indirectly lead to oxidations layers on the top of the film. For this reason, here in this work we aim to find a protecting

transparent surface that is known to be resistive to atmospheric variation. The effect of this binder on the performance of InSe will be investigated in this article.

In this work, we analyze, model and evaluate the optical conductivity parameters of GaSe/Binder. We expect that our results will be helpful in constructing new generation of optoelectronic devices.

Experimental Details

GaSe thin films were evaporated onto ultrasonically cleaned glass substrates from the source materials which are metal basis and Ga_2Se_3 (Alfa Aesar 12024-24-7 with maximum obtainable purity of 99.99%) single crystals. The evaporation was achieved in a VCM 600 physical vapor deposition system at vacuum pressure of 10^{-5} mbar. The thickness of $\sim 1.0 \mu\text{m}$ was controlled and measured using a thickness monitor attached to the VCM 600 evaporator. The amorphous nature of the GaSe films were reported in previous works (Schwarz et al., 2014; Kmail, and Qasrawi, 2015). A transparent thin film of sodium-based binder was poured onto the surface of GaSe film and left to dry for 24 hours. Previous studies revealed that this binder is mostly composed of $\text{Na}_2\text{O}_2 : \text{SiO}_2 : \text{CO}_3$ (Qasrawi, Sadreddin, 2016). The optical transmittance and reflectance were recorded using Evolution 300 spectrophotometer equipped with pike VEE MAX II variable angle reflectance accessory.

The optical conductivity was computed from the imaginary part of the dielectric constant. The dielectric constant was calculated from the reflectance and transmittance data in the wavelength range (300-1100 nm) using Fresnel's equations.

Results and discussion

Optically sensitive GaSe thin film coated with a sodium based binder, proves to be a fully transparent optical window.

Figure 1 (a) explores optical transmittance for the glass substrate in the incident light wavelength range of 300-1100 nm. We noticed high transmission ($\sim 90\%$) of the glass versus wavelength in the range of (300 – 1100 nm). Figure 1 (b) shows that the reflectance of the glass is negligible (< 1%) within the same wavelength range.

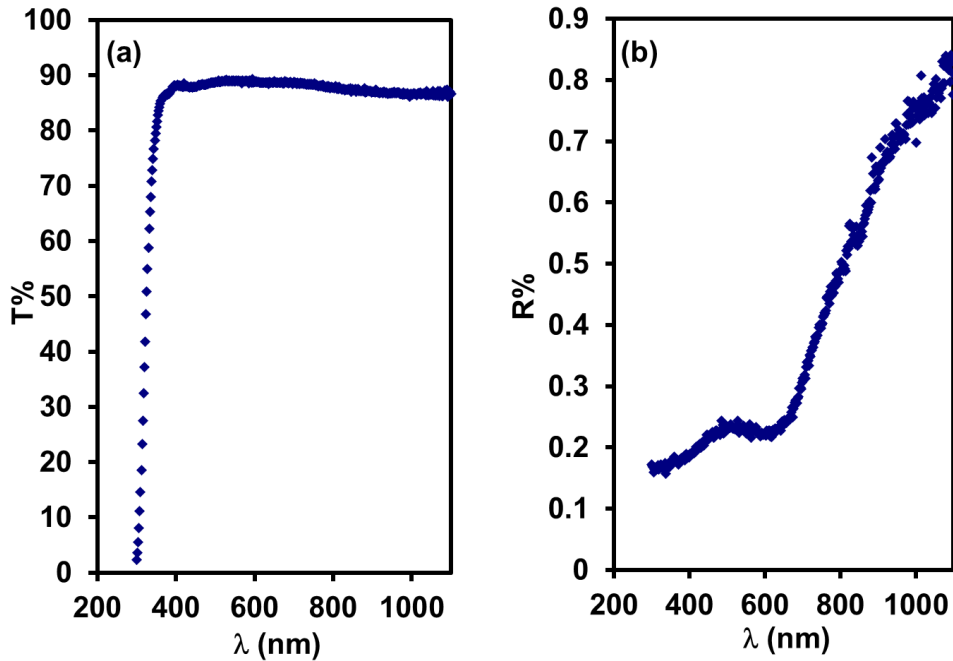


Fig. 1 The wavelength dependence of (a) the transmittance recorded at normal incidence and (b) the reflectance recorded at normal incidence for glass substrate.

Figure 2 (a) explores optical transmittance for the binder in the incident light wavelength range of 300-1100 nm. We noticed ~100 % transmittance of the binder versus wavelength in the range of (300 – 1100 nm). Figure 2 (b) shows that the reflectance of the binder is negligible (< 0.6 %) within the same wavelength range.

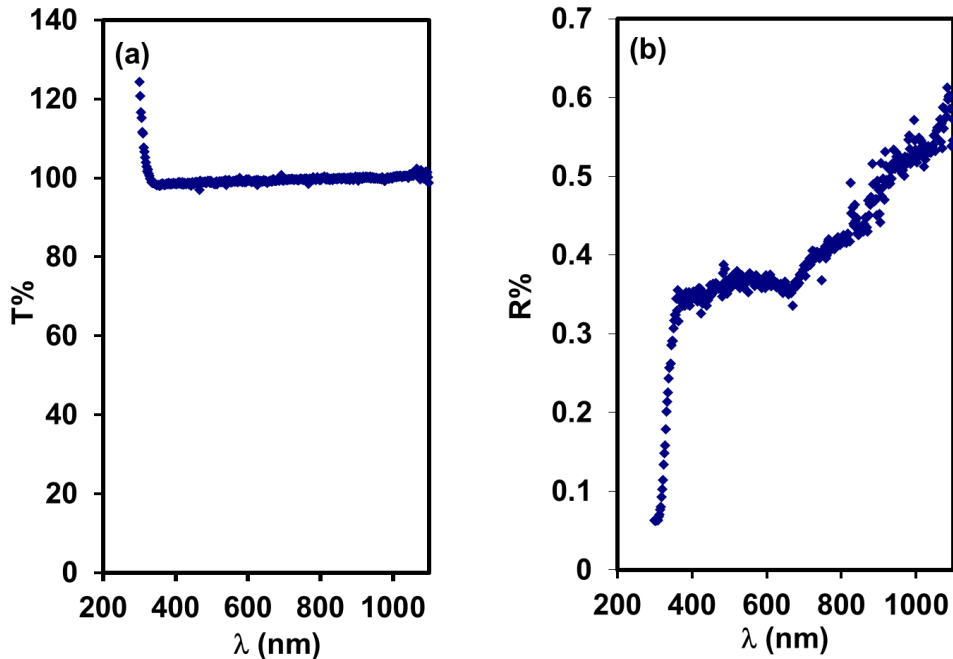


Fig. 2 The wavelength dependence of (a) the transmittance recorded at normal incidence and (b) the reflectance recorded at normal incidence for the binder.

Figure 3 (a) explores optical transmittance for the GaSe in the incident light wavelength range of 300-1100 nm. We noticed a sharp increase followed by a decrease in the transmittance of the GaSe versus wavelength in the range of (300 – 1100 nm). Figure 3 (b) clarifies a variation in the reflectance of the GaSe which is low (~3% - ~20%) within the same wavelength range.

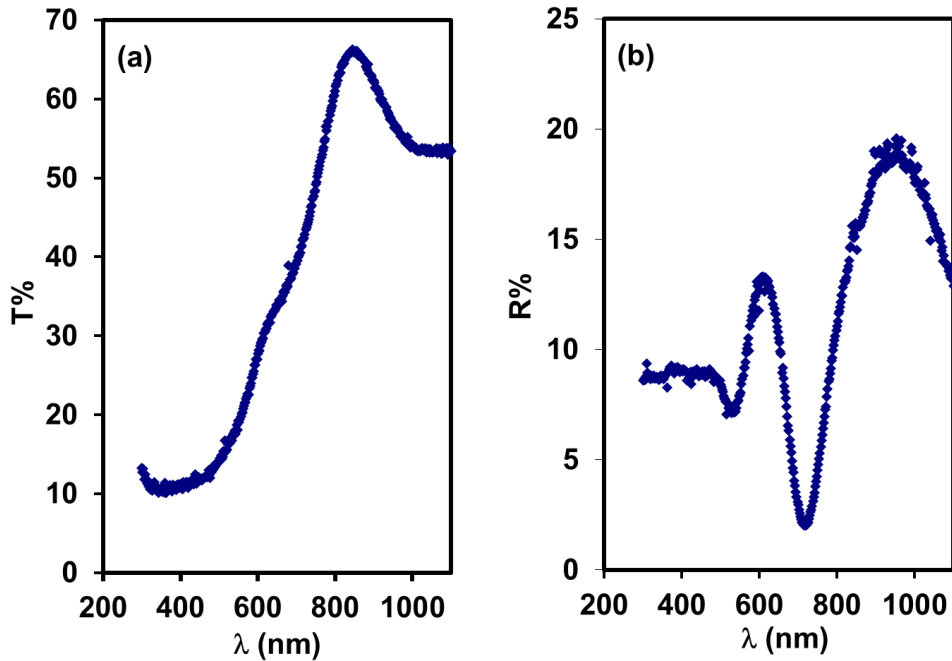


Fig. 3 The wavelength dependence of (a) the transmittance recorded at normal incidence and (b) the reflectance recorded at normal incidence for GaSe.

Figure 4 (a) explores optical transmittance for the GaSe/binder interfaces in the incident light wavelength range of 300–1100 nm. We noticed a sharp increase in the transmittance of the double layer versus wavelength in the range of (300 – 1100 nm). Figure 4 (b) clarifies that the reflectance of the double layer is very small within the same wavelength range. The peak shown at $\lambda=500$ nm (2.48 eV) in Fig 4(b) is due to an excitonic transition in GaSe which explains the origin of band gap in GaSe (Dey et all. 2015).

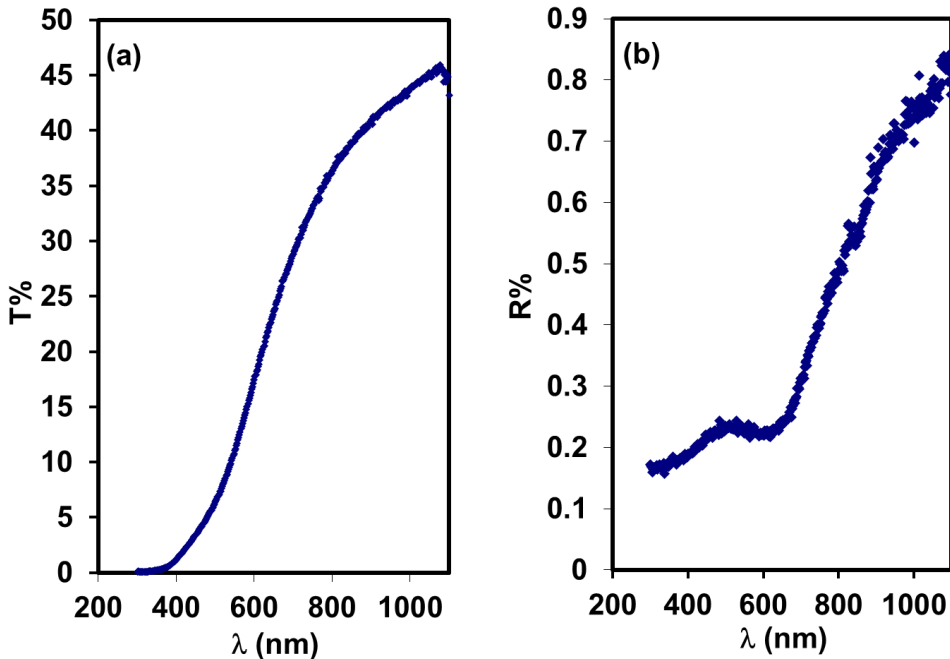


Fig. 4 The wavelength dependence of (a) the transmittance recorded at normal incidence and (b) the reflectance recorded at normal incidence for GaSe/Binder.

Figure 5 (a) shows that the absorption coefficient α of GaSe/Binder is directly proportional to the photon energy E within the range (1.16-3.2 eV), where α increases from 490 cm^{-1} to 853 cm^{-1} . The absorption coefficient α can be expressed by the equation (Pankove, 1971; Tauc, 1974).

$$\alpha = \frac{[B(E - E_g)^p]}{E} \quad (1)$$

Where B is a constant related to the transition probability, E_g is the band gap and p is an index that describes the optical absorption process and theoretically equal to 2, $\frac{1}{2}$, 3 or $\frac{3}{2}$ for indirect allowed, direct allowed, indirect forbidden and direct forbidden transitions respectively. To determine the value of the band gap, E_g , it is necessary to plot a graph of $(\alpha E)^{1/p}$ versus photon energy E , according to equation (1). For the applicable p , the linear portion of the graph can be extrapolated to find E_g from the intercept to the energy axis. Accordingly, the energy bandgap limit for GaSe/Binder thin film has been estimated for the only applicable value of $p=1/2$ by plotting $(\alpha E)^2$ versus photon energy E as shown in Fig. 5(b) . The intersection of the extrapolated linear portion belongs to the high absorption region of the curve, with horizontal axis (E) determines E_g ,

which shows that the energy bandgap of the GaSe/binder is approximately 1.6 eV (776.5 nm). This analysis revealed a pronounced red shift in the direct allowed electron transition's energy band gap of the GaSe and the reported band tail states of GaSe which was observed at ~ 0.25 eV disappeared upon binder coating.

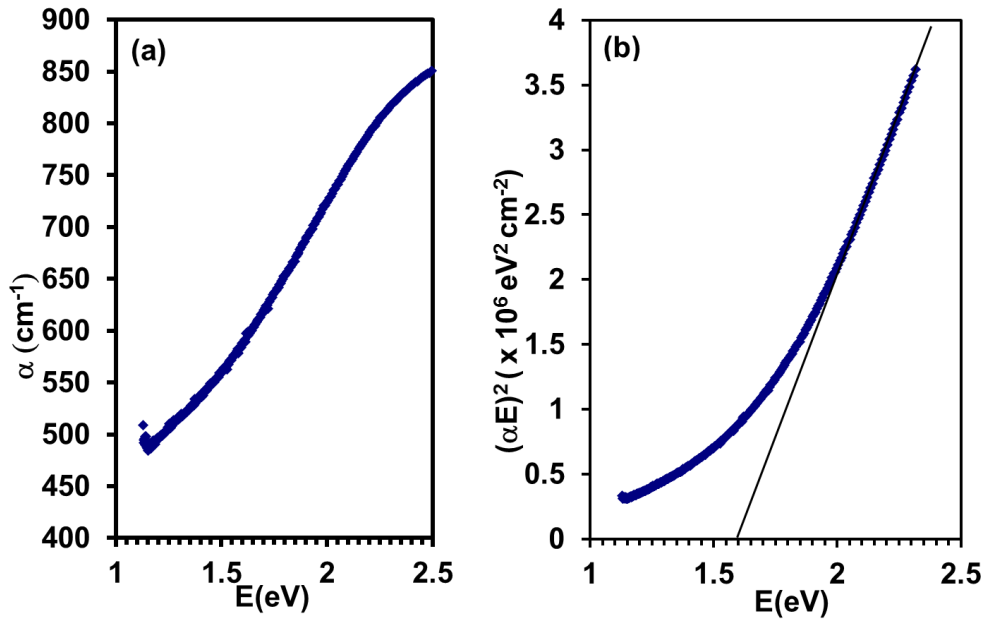


Fig. 5 (a) The $\alpha - E$ dependence for GaSe/Binder and **(b)** the $(\alpha E)^2$ dependence for Binder/GaSe.

Figure 6(a) shows the variation of the absorption coefficient α of GaSe alone with the photon energy E within the range (1.5-2.5 eV), where α varies between 2000 cm^{-1} to 7800 cm^{-1} . Figure 6(b) shows that the bandgap of GaSe alone is 1.85 eV.

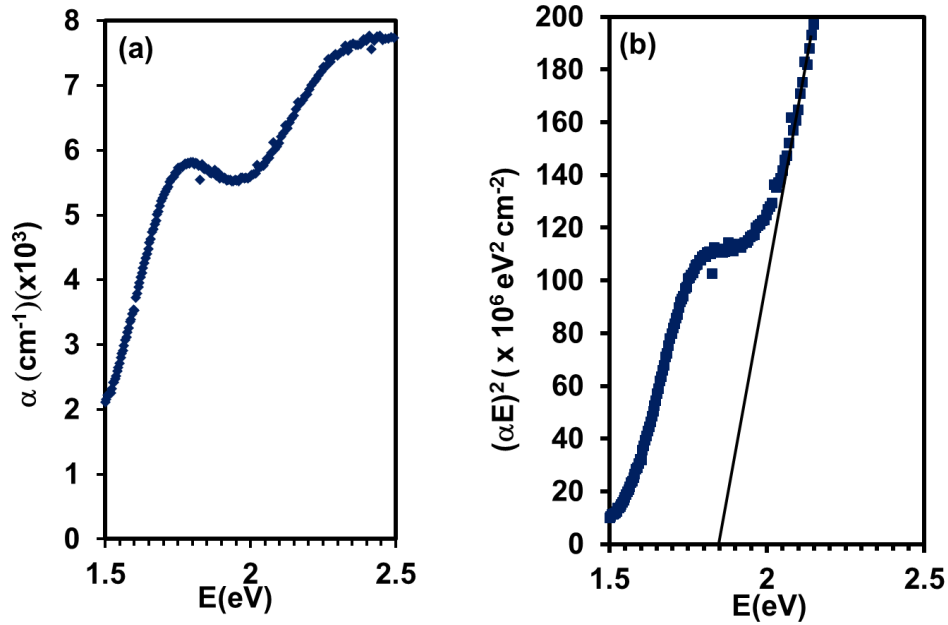


Fig. 6 (a) The $\alpha - E$ dependence for GaSe and **(b)** the $(\alpha E)^2$ dependence for GaSe.

Figure 7(a) shows the variation of the absorption coefficient α of the binder alone with the photon energy E within the range (1.0-2.5 eV), where $\alpha < 15 \text{ cm}^{-1}$. Figure 6(b) shows no evidence of a bandgap of the binder alone within the same photon energy range.

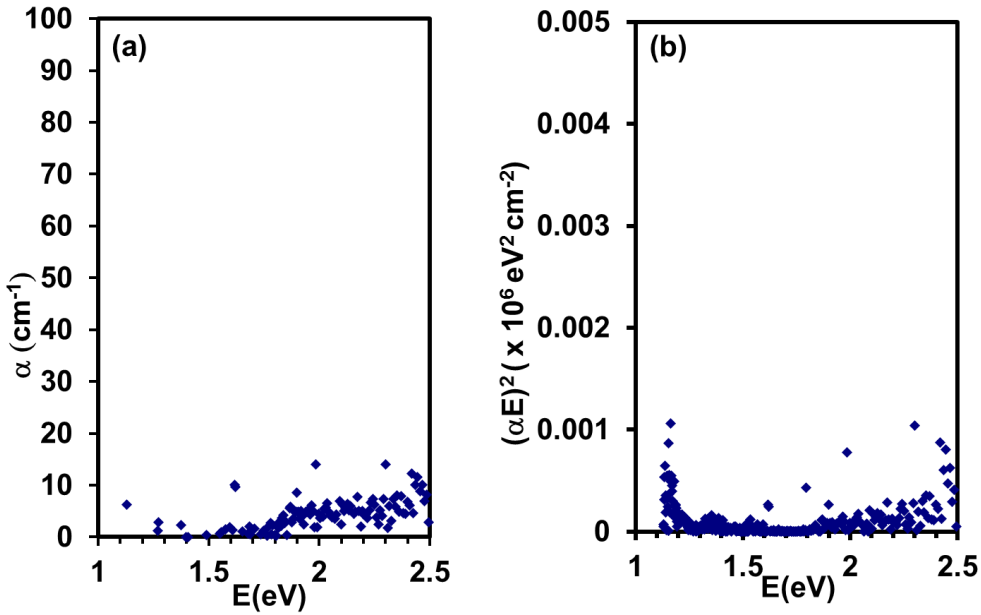


Fig. 7 (a) The $\alpha - E$ dependence for the Binder and **(b)** the $(\alpha E)^2$ dependence for the Binder.

Our data and the previous analysis show that the energy band gap difference $\Delta E_g = E_{g(\text{GaSe})} - E_{g(\text{GaSe/binder})} = 0.25 \text{ eV}$ is a sufficient value to design point contact devices.

On the other hand, Urbach clarifies that within the exponent edge where the absorption coefficient α lies in the absorption region of $1 < \alpha < 10^4 \text{ cm}^{-1}$, the absorption coefficient is given by equation (Urbach, 1953),

$$\alpha = \alpha_0 \exp\left(-\frac{E}{E_e}\right) \quad (2)$$

where α_0 is constant, E is the energy of incident photons and E_e is a characteristic energy representing the width of the Urbach tail states known to exist in disordered systems. Figure 8 shows a plot of $\ln(\alpha)$ versus E for $\alpha < 10^3 \text{ cm}^{-1}$. The slope of the best-fit is found to be 0.4306 eV^{-1} . Therefore $E_e = 2.32 \text{ eV}$, which shows that the width of the band tail states in the GaSe/Binder bilayer is 2.32 eV . Generally, band tails occur as a result of incomplete bonding between molecules at the surface or as a result of bonding between the atoms of binder with that of GaSe. Band tails are usually appears due to strained bonds in disordered systems.

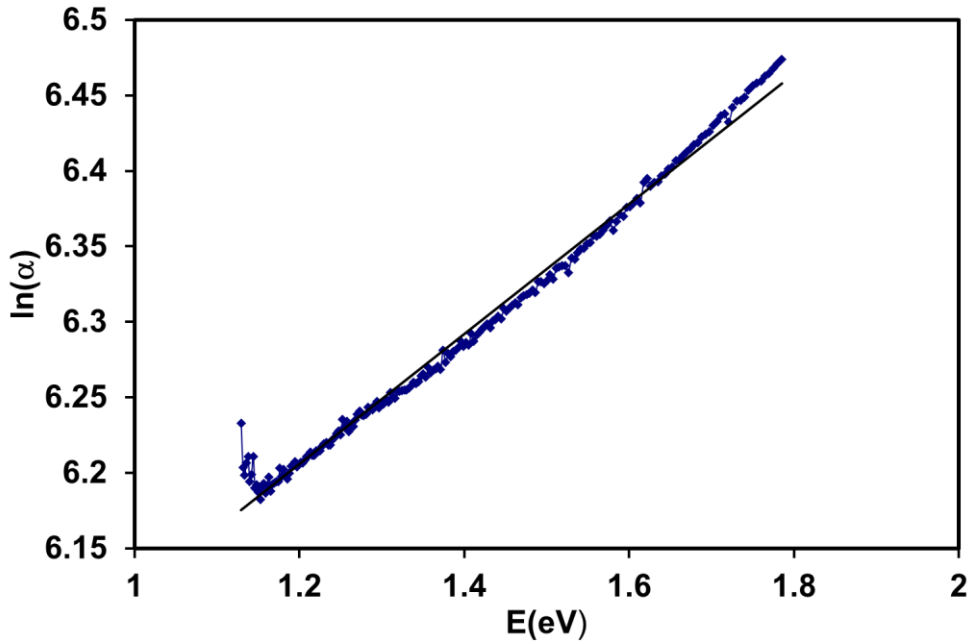


Fig. 8 The $\ln(\alpha)$ – E dependence for GaSe/Binder thin film.

To explore the possible applications of the GaSe/Binder structure, we studied its dielectric properties. The reflection (R) and extinction coefficient ($K = \frac{\alpha\lambda}{4\pi}$) data are used in evaluating the dielectric constant ($\epsilon = \epsilon_r + i \epsilon_{im}$) of the double layer thin film using the formula (Dresselhaus, 1980)

$$R = \frac{(n^2 - 1)^2 + K^2}{(n^2 + 1)^2 + K^2} \quad (3)$$

where n is the real part and K is the imaginary part of the refractive index. The real and imaginary parts of the dielectric constant are given by $\epsilon_r = n^2 - K^2$ and $\epsilon_{im} = 2nK$.

In Figure 9 (a) and (b) we present plots of both the real and the imaginary parts of the dielectric constant versus the photon frequency. Figure 9 (a) shows a sharp decrease followed by very slow variation then a slow decrease of ϵ_r with respect to photon's frequency in the frequency regions (280-460 THz, 461-700 THz, 701 – 1000 THz), respectively. The local maxima at 600

THz corresponds to an energy value of 2.486 eV. This number represents the direct allowed transitions energy band gap of GaSe (Dey et al, 2015). Below this value it decreasing according to the linear equation $\varepsilon_r = -3 \times 10^{-5} f + 1.1131$, due to the inability of electric dipole to orient with the oscillating electric field at these frequency values, leading to the freedom of some charged particles. Figure 9 (b) shows a sharp decrease followed by a slow decrease then a sharp decrease of ε_{im} with respect to photon's frequency in the frequency regions (270-470 THz, 471-550 THz, 551 – 1000 THz), respectively. The value of the imaginary part of the dielectric constant is very small compared with the real part.

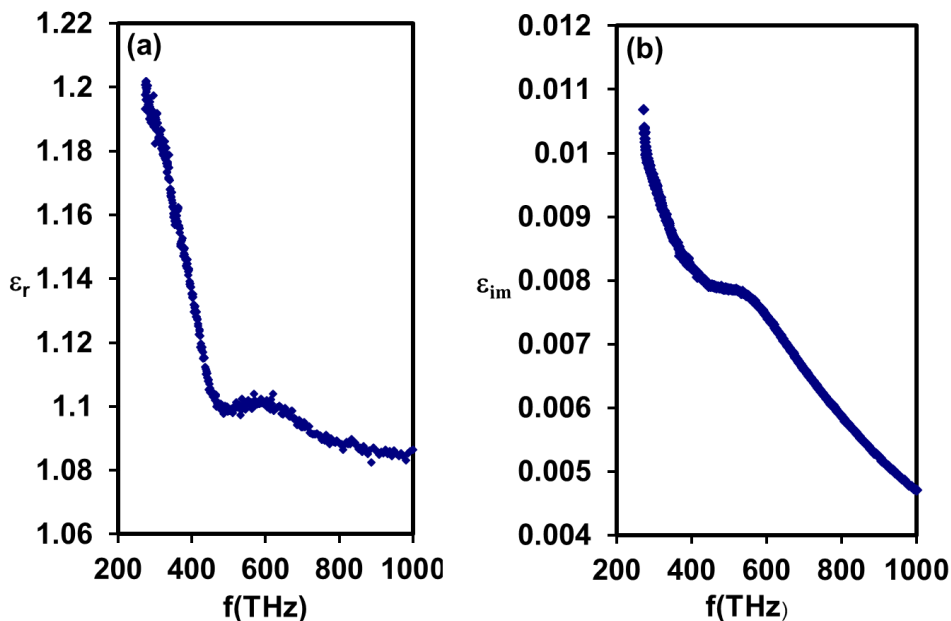


Fig. 9 (a) The frequency dependence of ε_r for GaSe/Binder and **(b)** The frequency dependence of ε_{im} for GaSe/Binder

To investigate the possible applications of this double layer as a thin film transistor, we used the relation $\sigma(\omega) = \frac{\varepsilon_{im}\omega}{4\pi}$ to evaluate the optical conductivity of the GaSe/Binder double layer, where ω is the angular frequency. It is worth noting that the conductivity variations are directly proportional with the imaginary part of the dielectric constant. The σ spectra are shown in Fig. 10.

We modeled the variation in the optical conductivity σ according to Lorentz model, which clarifies the behavior of bounded electrons in an atom in solids. According to Lorentz model (Pankove, 1971), the relation expresses the optical conductivity is given by

$$\sum_{k=1}^2 \sigma_k(\omega) = \frac{\omega_{pe_k}^2 \omega^2 \gamma_k / 4\pi}{(\omega_{e_k}^2 - \omega^2)^2 + \omega^2 \gamma_k^2} \quad (4)$$

where k is an index that represent the number of oscillators and $k=1,2$ oscillators are assumed to exist, $\omega_{pe} = \sqrt{4\pi n e^2 / m^*}$ is the bound electron plasma frequency, $\gamma = \tau^{-1}$, τ is the electron scattering time, ω_e is the reduced resonant frequency, which deals with the effects of the local fields on the optical conductivity.

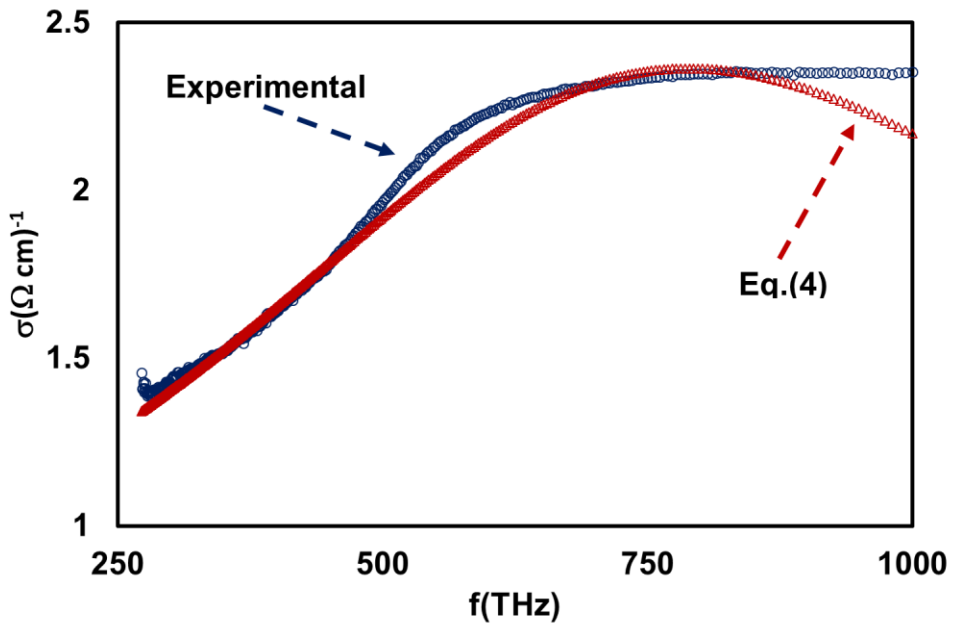


Fig. 10 The frequency dependence of optical conductivity for GaSe/Binder.

Equation (4) includes the frequency free conductivity $\sigma_{dc} = ne^2\tau/m^* = ne\mu$ where μ and m^* are the drift mobility and the effective mass, respectively. The following table summarizes the fitting parameters substituted in Eq. (4) to evaluate the optical conductivity σ and plotted in Fig. (10):

Table 1. The fitting parameters of the imaginary part of the dielectric constant of GaSe/Binder

Parameters	K=1	K=2
$\tau(\text{fs})$	0.137	0.132
m^*/m_0	0.3	0.3
$n(\text{cm}^{-3})$	1.11×10^{18}	7.37×10^{17}
$\omega_e(\text{rad/s})$	5.33×10^{15}	1.70×10^{15}
$\sigma_{dc}(\Omega \text{ cm})^{-1}$	0.14	0.09
$\mu(\text{cm}^2/\text{Vs})$	0.8	0.77
$\omega_{pe}(\text{GHz})$	1.14	0.93

The optical conductivity displayed significant change in the free carrier density, the drift mobility, the electron collision time and the effective mass for GaSe upon binder coating as shown in Table (1) compared to that reported by Qasrawi (Qasrawi et al., 2016). Particularly, the change in the scattering time appears to be insignificant indicating that the damping coefficient (τ^{-1}) or the so-called electronic friction is constant. Increasing the electron oscillation frequency is associated with increased free electron density as shown in our table. Remarkable change by one order of magnitude is observed in the free carrier density. That increase causes an increase in the electrical conductivity and invariant drift mobility. Similarly, the electron bound plasmon frequency shifts from 0.93 MHz to 1.140 GHz. The latter value indicate that all AC signals of frequencies less than 1.14 GHz are rejected, while those of 1.14 are in resonance with the free electrons of metal and signals of higher frequencies are transmitted. Such property means that the GaSe/binder bilayer is very attractive for use as band pass/reject filters at Gigahertz frequencies. Physically, the surface plasmons which are coherent delocalized electron oscillations that exist at the interface between GaSe and binder where the dielectric function changes sign across the interface have lower energy than bulk plasmon which quantize the longitudinal electron oscillations about positive ion cores within the bulk of an electron gas (or plasma). As the surface plasmon propagates along the surface, it loses energy to the metal due to absorption.

Conclusions

In our work, 1 μm of amorphous n-type GaSe thin film is coated with 10 μm of sodium based binder. The optical features of the bilayer which is determined through energy band gap analysis have shown wide absorbability that extends from 2.48 to 1.50 eV. The absorption ability increased due to the presence of GaSe and this may be useful for using the GaSe/Binder for photovoltaic applications. Such values are attractive for photovoltaic applications. The dielectric spectra for those films clarifies distinguished optical properties characterized by the enhanced optical conductivity and dielectric values. The scattering time of GaSe/Binder thin film at femtosecond and the plasmonic behavior near 1 GHz make it suitable for usage in microwave based electric devices. Particular application of this bilayer is tested through optical conductivity and it was shown that such device, which is regarded as plasmonic device, can oscillate, reject and transmit signal at 1.14 GHz.

References

1. Qasrawi, A. F. (2005), Refractive index, band gap and oscillator parameters of amorphous GaSe thin films. Cryst. Res. Technol. **40**, No. 6, PP 610-614.
2. Qasrawi, A. F., Sadeddin, Iyad A., Attieh, Alghamdi, A. and N. M. Jaradat, Haneen (2016), Mechanical Properties and Effect of the MgO Content on the Dielectric Breakdown in the MgO/Binder Mixtures. Journal of Materials Science and Engineering **B 5 (1-2)**, PP 48-53.
3. Toullec, R. Le , Piccioli, N. and Chervin, J. C. (1980), Optical properties of the band-edge exciton in GaSe crystals at 10 K, Phys. Rev. B **22**, PP 6162.
4. Shigetomi, S. and Ikari, T. (2003), Optical properties of GaSe grown with an excess and a lack of Ga atoms, J. Appl. Phys. **94**, PP 5399.
5. Allakhverdiev, K. R., Yetis, M. Ö., Özbek, S., Baykara, T. K. and Salaev, E. Yu. (2009), Effective nonlinear GaSe crystal. Optical properties and applications, Laser Physics, **19**, issue 6, PP 1092-1104.
6. Schrieffer, J. R. (2007), Hand Book of High-Temperature Superconductivity: Theory and Experiment, Springer, New York, NY.

7. Qasrawi, A. F., Khanfar, Hazem K. and Kmail, Renal R. N. (2016), Optical conduction in amorphous GaSe thin films, *Optik* **127**, PP 5193-5195.
8. Schwarz, S., Dufferwiel, S., Walker, P.M., Withers, F., Trichet, A.A.P., Sich, M., Li, F., Chekhovich, E.A., Borisenko, D.N., Kolesnikov, N.N., Novoselov, K.S., Skolnick, M.S., Smith, J.M., Krizhanovskii, D.N., Tartakovskii, A.I. (2014), Two-dimensional metalechalcogenide films in tunable optical microcavities, *Nano Lett.* **14**, PP 7003-7008.
9. Kmail, R.R.N., Qasrawi, A.F. (2015), Physical Design and Dynamical Analysis of Resonant–Antiresonant Ag/MgO/GaSe/Al Optoelectronic Microwave Devices, *J. Electron. Mater* **44**, PP 4191-4198.
10. Dey, P., Paul, J., Moody, G., Stevens, C. E., Glikin, N., Kovalyuk, Z. D., Kudrynskyi, Z. R. et al (2015). Biexciton formation and exciton coherent coupling in layered GaSe, *The Journal of chemical physics* 142, no. 21, P 212422.
11. Pankove, J. I. (1971), *Optical Processes in Semiconductors*, Prentice-Hall, New Jersey.
12. Tauc, J. (1974), “Amorphous and liquid semiconductors”, New York, PLENUM, ch. 4.
13. Urbach, F. (1953), The Long-Wavelength Edge of Photographic Sensitivity and of the Electronic Absorption of Solids, *Phys. Rev.* **92**, P1324.
14. Dresselhaus, M. (1980), *Optical Properties of Solids*, American Scientific Publishers, New York, NY.

تأثير المواد الرابطة الشفافة القائمة على الصوديوم في الخصائص البصرية لأغشية GaSe الرقيقة

احمد عمر

قسم الفيزياء، الجامعة العربية الأمريكية - فلسطين

ahmad.omar@aauij.edu

الملخص

تم استكشاف تأثير المواد الرابطة الشفافة القائمة في الصوديوم على الخصائص البصرية لأغشية $GaSe$ الرقيقة المبخرة فراغياً بواسطة الانعكاسية والنفاذية البصرية للمادة الرابطة، بالإضافة إلى السطوح البينية لكل من $GaSe$ و $GaSe/GaSe$ الرابط تحت تأثير ضوء ساقط في مدى الطول الموجي 300 - 1100 نانومتر. لقد أظهرت تحليلات طيف معامل الامتصاص للعينات الثلاثة عن وجود تحول واضح نحو منطقة الطيف الأحمر في منطقة السماح المباشر لانتقال الإلكترون خلال فجوة نطاق الطاقة لمادة $GaSe$. بالإضافة إلى ملاحظة أن حالات ذيل النطاق لمادة $GaSe$ والتي لوحظت عند حوالي 0.25 eV قد اختفت بعد طلائها بالمادة الرابطة. وقد تسبب طلاء المادة الرابطة فوق مادة $GaSe$ بازهار الفجوة في نطاق طاقة آل $GaSe$ حالة ذيل النطاق داخل فجوة نطاق طاقته. ومن ناحية أخرى، بينت تحليلات طيف المادة العازلة للغشاء الرقيق لمادة $GaSe$ المطلية بالمادة الرابطة وجود تحسينات غير طبيعية على الموصلية البصرية للطبقة المزدوجة. وقد أظهرت الموصلية البصرية، التي تم تصميم نموذج خاص بها وفقاً لنظرية لورنتز، تغيراً كبيراً في كثافة الناقل الحر، وتقل الانحراف، ووقت اصطدام الإلكترون والكتلة الفعلية لـ $GaSe$ بعد طلائه بالمادة الرابطة.

وانتهت الدراسة بنتيجة مفادها أن الرابط القائم على الصوديوم يتصرف كنافذة بصرية شفافة تماماً للأغشية الرقيقة لمادة $GaSe$ الحساسة كهروضوئياً.

الكلمات الدالة: الموصلية البصرية، الرابط، الطلاء، $GaSe$